

Effect of Chemical Interaction Between Surface Oxidized Carbon Black and Carboxylated Nitrile Rubber on Dynamic Properties

SUMANDA BANDYOPADHYAY, P. P. DE, D. K. TRIPATHY, and S. K. DE*

Rubber Technology Centre, Indian Institute of Technology, Kharagpur 721 302, India

SYNOPSIS

Monsanto rheometric, dynamic mechanical, and solvent swelling studies indicate that functional groups of oxidized carbon black chemically react with carboxylated nitrile rubber (XNBR) when heated at high temperature for prolonged time. The reinforcing ability of the surface oxidized carbon black, measured by failure and hysteresis properties, is higher than the nonoxidized counterpart. © 1995 John Wiley & Sons, Inc.

INTRODUCTION

Chemical reactivity of rubber grade furnace blacks is attributed to the presence of several functional groups on the surface of carbon black.¹⁻³ Oxygen-containing functional groups include carboxyl, lactone, phenol, and quinone.⁴ Although morphology of carbon black and, in particular, its surface area play important roles in rubber reinforcement as compared to the chemical energy available at the filler surface,⁵ chemical interaction between carbon black and rubber contributes to high reinforcement in many instances.⁶ Gessler showed that surface oxidized carbon blacks impart high reinforcement in butyl rubber when heated at high temperature.⁷ Asai and co-workers reported that oxidative treatment of carbon black caused increased reinforcement in natural rubber-carbon black system.⁸ The chemical nature of the surface energy in carbon black is expected to be more important in the case of polar rubbers. Wang and co-workers showed that polar rubbers like nitrile rubber exhibit stronger interaction with carbon blacks as compared to the nonpolar olefinic rubbers.⁴ It is believed that polar rubbers with reactive functional groups contribute more toward the rubber-filler interaction than the cor-

responding nonpolar rubbers. The role of carbon black surface chemistry in the reinforcement of polar rubbers has not been studied in detail. Recently, Roychoudhury et al. reported that oxidized carbon black chemically reacts with epoxidized natural rubber and chlorosulfonated polyethylene, the extent of the reaction being dependent on the concentration of oxygen-containing functional groups on the carbon black surface.^{9,10}

This paper deals with the interaction between carbon black and carboxylated nitrile rubber (XNBR). The study includes different grades of carbon black with varying concentrations of oxygen-containing groups on the carbon black surface.

EXPERIMENTAL

Details of the materials used are given in Table I and formulations of the different rubber mixes are given in Table II. Mixing of the fillers with rubber was done in a Brabender Plasticorder (Model PLE-330) at room temperature and at a rotor speed of 60 rpm for 8 min. The equipment was fitted with a cam-type mixing head and mixing was done at a constant input energy.

For determination of bound rubber, the rubber-carbon black mixes were conditioned at room temperature and then cut into small pieces (1 mm² area) which were immersed in 300 mL of chloroform for

* To whom correspondence should be addressed.

Table I Details of Materials Used

Material	Characteristics	Source
Carboxylated nitrile rubber (XNBR) KRYNACK \times 7.50	% acrylonitrile = 27 % carboxyl = 7 Mooney viscosity (ML1 + 4) at 100°C, 50	Bayer Polysar, France
Channel black (Gasru β CK 3)	DBP: 108 mL/100 mg N ₂ SA: 100 m ² /g pH: 4.0, %O: 3.1	Degussa AG, Germany
Oxidized ISAF black (Spezialschwarz-550)	DBP: 47 mL/100 mg N ₂ SA: 110 m ² /g pH: 2.8, %O: 1.44	Degussa AG, Germany
ISAF black (Printex-55)	DBP: 45 mL/100 mg N ₂ SA: 105 m ² /g pH: 9.5, %O: 0.9	Degussa AG, Germany
SRF black	DBP: 70 mL/100 mg N ₂ SA: 20 m ² /g pH: 7.5, %O: 0.2	Phillips Carbon Black Ltd., India

24 h. The insolubilized sample was extracted at room temperature and then vacuum dried to constant weight. The bound rubber content was expressed as the weight percent of the insolubilized rubber remaining on the black.

Rheometric studies of the rubber-carbon black mixes (Table II) were carried out at 190°C in a Monsanto R-100 rheometer at 3° arc of oscillation. Molding of the rubber-carbon black mixes was done at 190°C for 60 min under 10 MPa pressure in a

hydraulic press. For mix number 1 in Table II molding was done at different times (2, 30, and 60 min).

The molded samples were allowed to swell in chloroform at room temperature for 72 h to achieve equilibrium swelling and the results are expressed as percent weight loss of the sample. The stress-strain properties were measured as per ASTM D-412-87 in a Zwick Universal Testing Machine (Model 1445). The abrasion resistance of the samples was measured as per BS:903:Part A9:1957—Method C in a Dupont Abrasion Tester. The hysteresis measurements were carried out with a dumb-

Table II Formulations of the Rubber-Carbon Black Mixes Along with the Corresponding Bound Rubber and Monsanto Rheometric Torque Rise

Material	Mix Number			
	1	2	3	4
XNBR	100	100	100	100
Channel black	75	—	—	—
Oxidized ISAF black	—	75	—	—
ISAF black	—	—	75	—
SRF black	—	—	—	75
Bound rubber (%)	23	18	15	10
Rheometer torque rise, Δt^a (dN-m)	19	13	10	6

* Difference between the measured torque at 60 min and the minimum torque at 190°C.

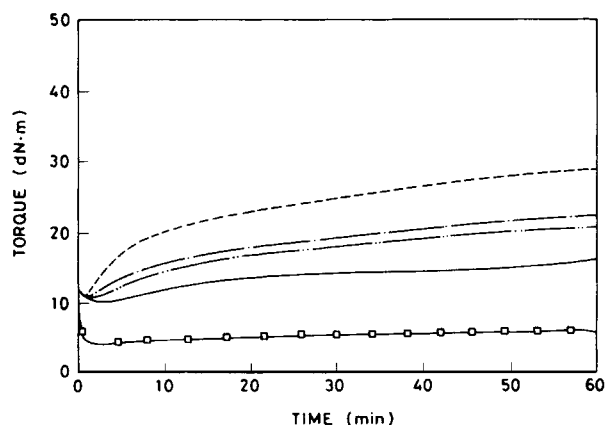


Figure 1 Monsanto rheographs at 190°C of (-----) XNBR-channel black; (---) XNBR-oxidized ISAF black; (- · - ·) XNBR-ISAF black; (—) XNBR-SRF black (—□—) neat XNBR.

bell-shaped test specimen as per ASTM D-412-80 in a Zwick Universal Testing Machine (model-1445) at 100% elongation for two consecutive cycles. The dynamic mechanical properties were studied using a Rheovibron (Model DDV-III-EP, Orientec Corp., Japan) at a double strain amplitude of 0.166% and a frequency of 3.5 Hz. The temperature scan was made from -100 to $+200^{\circ}\text{C}$. The procedure was to cool the samples to -100°C using liquid nitrogen and then an equilibrium linear rise of $2^{\circ}\text{C}/\text{min}$ was allowed.

The low strain dynamic mechanical studies of the molded samples were made in a Rheovibron, DDV-III-EP (Orientec Corp., Japan) at room temperature under tension mode. The double strain amplitude (DSA) was varied from 0.083 to 5% and the frequency was kept constant at 3.5 Hz. DSA is defined as $(2 \times A)/L$, where A is the amplitude of vibration and L is the length of the sample.

RESULTS AND DISCUSSION

Figure 1 shows the Monsanto rheographs of different mixes. In the case of XNBR-carbon black mixes, the rheographs were taken at 190°C because the torque rise was low at lower temperature. Table II summarizes the results of the rheometric studies. In

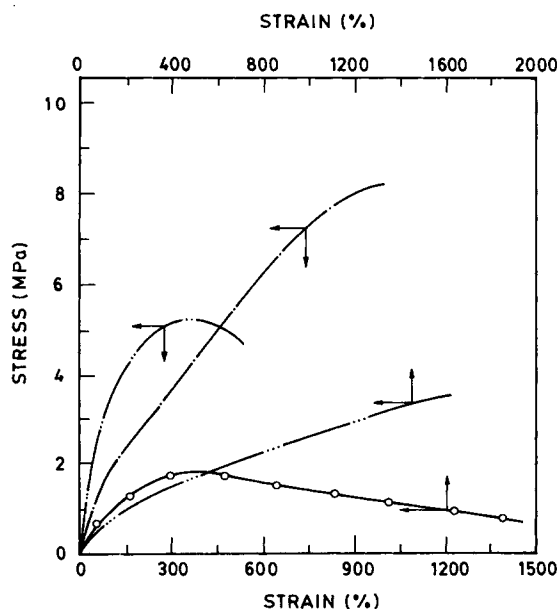


Figure 2 Stress-strain properties of XNBR-carbon black systems molded at 190°C for 60 min: (— · · —) channel black; (— · —) oxidized ISAF black; (— · · · —) ISAF black; (— ○ —) SRF black.

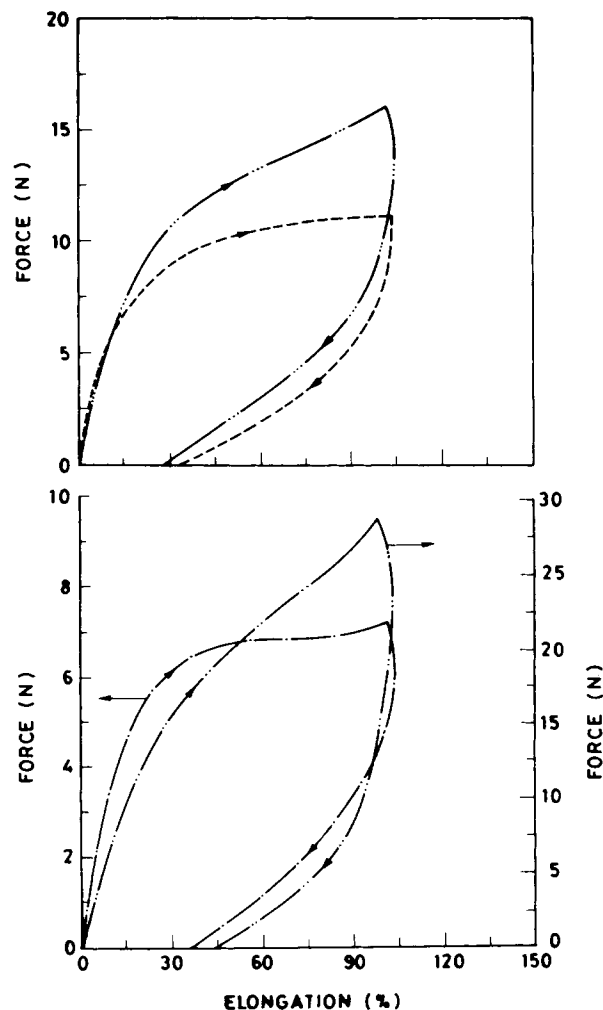


Figure 3 Hysteresis loops of XNBR-carbon black systems molded at 190°C for 60 min: (— · · —) channel black; (— · · · —) oxidized ISAF black; (— · · —) ISAF black; (— ○ —) SRF black.

the case of neat polymer (XNBR), Δt (the difference in torque rise between the measured torque at 60 min and the minimum torque) is very low, thus eliminating the possibility of thermovulcanization. In the case of XNBR-carbon black mixes, the SRF black registers the minimum torque rise and the channel black registers the maximum torque rise. For the two grades of ISAF carbon black, the oxidized grade registers higher torque rise than the corresponding nonoxidized grade. The Δt values follow the order, XNBR-channel black > XNBR-oxidized ISAF black > XNBR-nonoxidized ISAF black > XNBR-SRF black. The percent oxygen present on the surface of the carbon black (Table I) follows the order, channel black > oxidized ISAF black > nonoxidized ISAF black > SRF black. It is, there-

fore, apparent that a correlation exists between the oxygen concentration on the carbon black surface and the extent of rheometric torque rise. If the increase in rheometric torque is attributed to the crosslinking of the rubber, then weight loss on swelling is maximum for XNBR-SRF carbon black and is minimum for XNBR-channel black. The oxidized ISAF black shows values close to the channel black but less than the corresponding ISAF black. Since the extent of crosslinking is inversely proportional to percent weight loss on solvent swelling, the results correlate well with the Δt values of the rheometer studies.

Figure 2 shows the stress-strain behavior of different XNBR-carbon black mixes molded at 190°C for 60 min. The results of stress-strain studies are summarized in Table III. While mixes containing SRF and ISAF carbon blacks register low tensile strength, those containing oxidized ISAF black show high tensile strength. The mix containing channel black shows yielding and registers low tensile strength. The tear strength results are also shown in Table III. It is observed that the tear strength results also follow the same order as the Δt values in the rheometer studies.

Figure 3 shows the hysteresis plots of different XNBR-carbon black mixes molded at 190°C for 60 mins. The results are summarized in Table III. It is apparent that the hysteresis loss runs parallel with the tear strength. Abrasion loss also follows a similar order. Here two factors are operative: (1) crosslinking of XNBR through chemical interaction between rubber and carbon black and (2) the reinforcing effect of the filler particles in the rubber phase. Although, in the present case, there is an increase in the extent of chemical interaction in the order,

XNBR-channel black > XNBR-oxidized ISAF black > XNBR-ISAF black > and XNBR-SRF black, hysteresis loss also follows the same order. Increase in chemical interaction or bonding is supposed to cause decrease in hysteresis loss, which, however, does not happen in the present case. It appears, therefore, that the effect of chemical interaction between XNBR and the filler particles is overshadowed by the reinforcing ability of the filler particles. The bound rubber is known to play a major role in the reinforcement of elastomers^{11,12} and surface oxidation of carbon black caused increase in bound rubber in XNBR (Table II).

Figure 4 shows the variation of storage modulus (E'), loss modulus (E'') and loss tangent ($\tan \delta$) with temperature for different XNBR-carbon black systems. Plots of E' and E'' at room temperature against percent oxygen concentration on the filler surface are shown in Figure 5a. It is evident that both E' and E'' at room temperature follow the order, XNBR-SRF black < XNBR-ISAF black < XNBR-oxidized ISAF black < XNBR-channel black, but the rate of increase of E' is higher than that of E'' . While increase in E'' may be ascribed to the physical bonding between rubber and filler leading to reinforcement, increase in E' is ascribed to both reinforcement and chemical bonding between rubber and filler.^{13,18} Figure 5b shows the plots of $(\tan \delta)_{\max}$ (that is, $\tan \delta$ value at T_g) against percent oxygen on the filler surface. It is apparent that $(\tan \delta)_{\max}$ gradually decreases with increase in oxygen concentration, but the rate of decrease is less at high concentration. Lowering of $\tan \delta$ at T_g is believed to be due to both chemical crosslinking of the polymer chains and polymer-filler interaction.^{13,18,19} In the present system both weak physical bonding and strong chemical

Table III Physical Properties of the Molded Samples of XNBR-Carbon Black Mixes

Properties	Mix Number			
	1	2	3	4
100% modulus (MPa)	3.33	2.94	1.26	1.37
300% modulus (MPa)	5.03	3.67	1.60	1.82
Tensile strength (MPa)	4.48	8.11	3.33	0.94
Elongation at break (%)	489	988	1682	1970
Tear strength (N/mm)	39.1	32.0	21.9	17.2
Hardness (Shore A)	70	60	55	51
Hysteresis loss $\times 10^3$ (J/m ²)	79	46	36	32
Abrasion loss (cm ³ /h)	0.12	0.16	0.28	0.38
% weight loss on swelling in chloroform	47	49	61	76

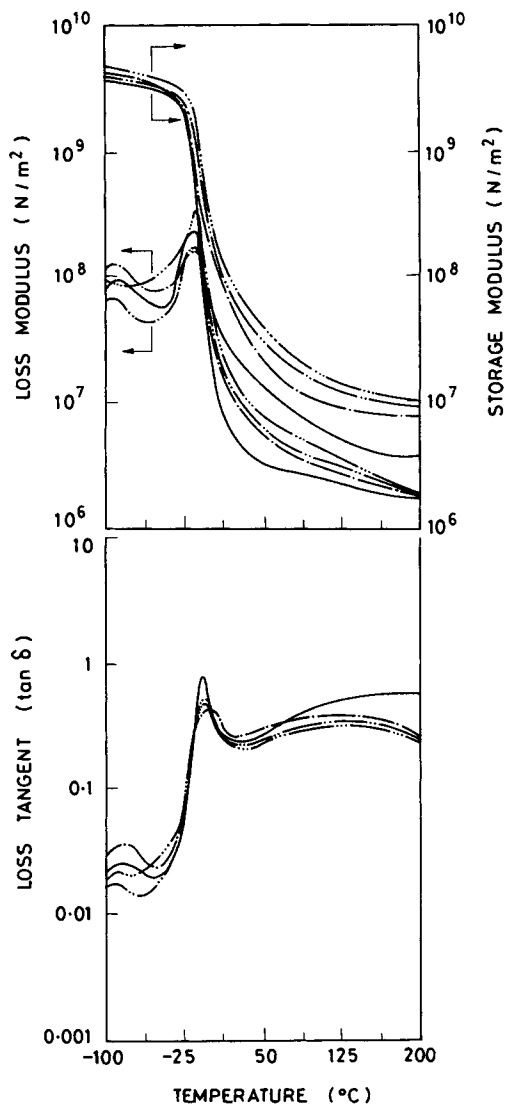


Figure 4 Temperature dependence of dynamic mechanical properties of XNBR-carbon black systems molded at 190°C for 60 min: (— · · · —) channel black; (— · · —) oxidized ISAF; (— · —) ISAF black; (—) SRF black.

bonding are responsible for lowering of $(\tan \delta)_{\max}$ on incorporation of filler. Figure 6 shows the effect of molding time on dynamic mechanical properties. With increase in molding time, E' gradually increases and the $\tan \delta$ at T_g gradually decreases, indicating involvement of carbon black surface in crosslinking of the rubber phase.¹³⁻¹⁸ The $\tan \delta$ shows a broad maxima at high temperature, which is believed not to be due to any transition in XNBR. The rate of decrease in E'' at high temperature is more than that of E' , causing an increase in $\tan \delta$. Beyond the broad maxima, the $\tan \delta$ decreases because E'

gradually increases due to additional crosslinking during measurement at high temperature and the rate of increase of E' is more than the changes in E'' . Furthermore, with increase in molding time, extent of additional crosslinking during prolonged testing decreases, which causes the gradual disappearance of the broad maxima in $\tan \delta$ at high temperature.

A typical plot for the variation of the in-phase storage modulus with percent DSA for different XNBR-carbon black mixes is shown in Figure 7a. Results are summarized in Table IV. The storage modulus decreases with increasing DSA. The difference $\Delta E'$ [that is, $(E'_0 - E'_a)$, where E'_0 is the storage modulus value at low strain (0.083%) and E'_a is the value at high strain (5%)] is believed to be due to structure breakdown of the carbon-carbon net-

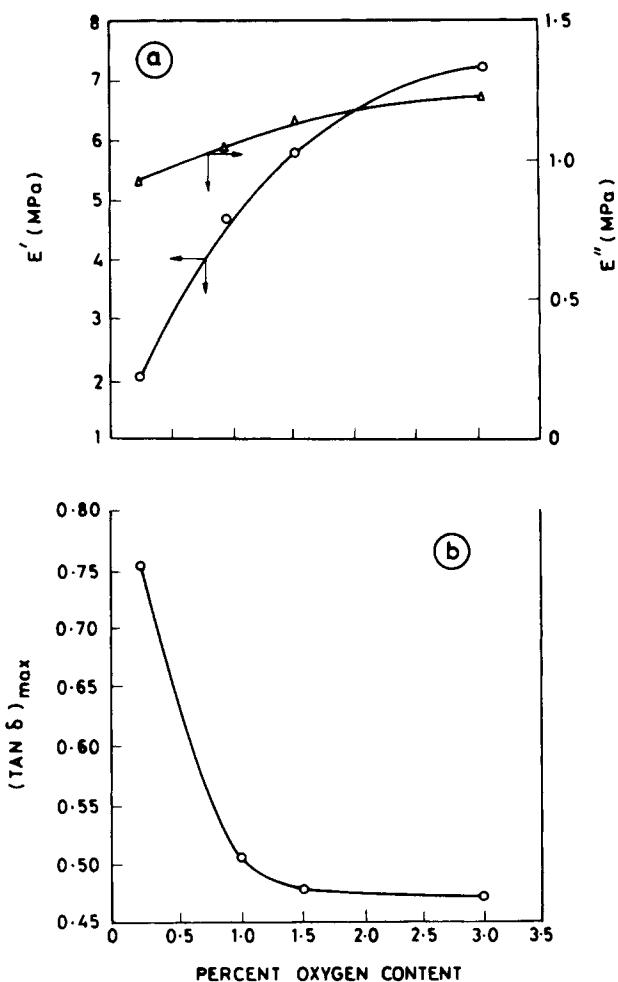


Figure 5 (a) Effect of percent oxygen on the carbon black surface on E' and E'' of XNBR-carbon black system. (b) Effect of percent oxygen on the carbon black surface on the $(\tan \delta)_{\max}$ of XNBR-carbon black system.

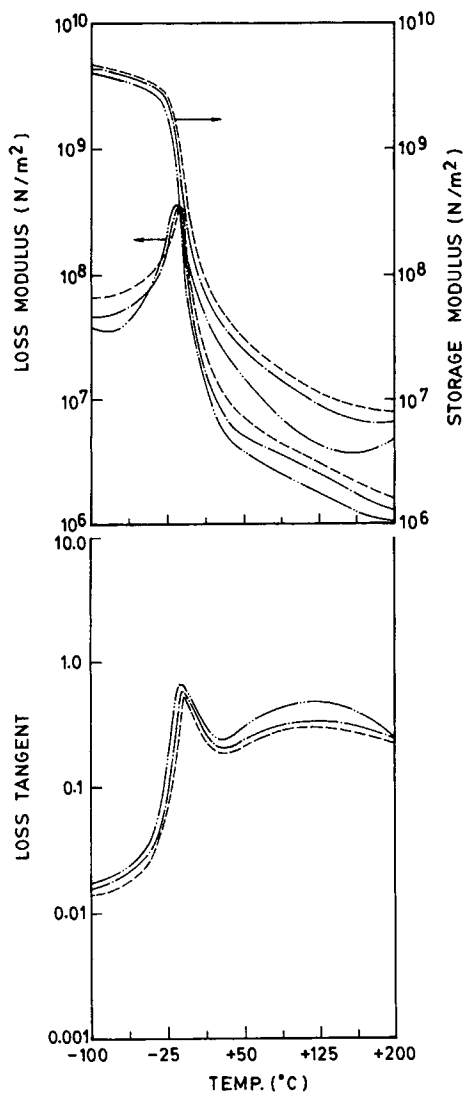


Figure 6 Effect of molding time on the temperature dependence of dynamic mechanical properties of XNBR-channel black system (Mix No. 1 of Table II), molded at 190°C: (— · —) 2 min; (— · —) 30 min; (---) 60 min.

work system or interaggregate.^{15-17,20,21} Since $\Delta E'$ is less for the oxidized carbon black, it is apparent that there is a reduction in interaggregate formation of the filler particles which interact chemically with the rubber matrix and form rubber-filler network. When subjected to dynamic strain, most of the filler-filler interaggregates and part of the rubber-filler network undergo breakdown. In the case of ISAF carbon black filler, the rubber-filler network formation is less as compared to the oxidized counterpart. Accordingly, extent of filler-filler interaggregate formation and subsequent breakdown on application of dynamic strain is more and $\Delta E'$ is higher

as compared to the corresponding oxidized filler. Rubber-filler interaction is minimum in the case of SRF carbon black and, furthermore, E' values at both high and low strains are very low in this case, and so the $\Delta E'$ value is the minimum among the different carbon blacks studied. Figure 7b shows variation in E' with percent DSA in the case XNBR-channel black system at different molding times. The results are summarized in Table V. Increase in molding time causes increase in extent of chemical bonding. This increases the low strain modulus of the sample but causes a reduction in $\Delta E'$.

Recently Ayala et al.²² proposed a rubber-filler interaction parameter, I , which is defined as

$$I = \sigma/\eta \quad (1)$$

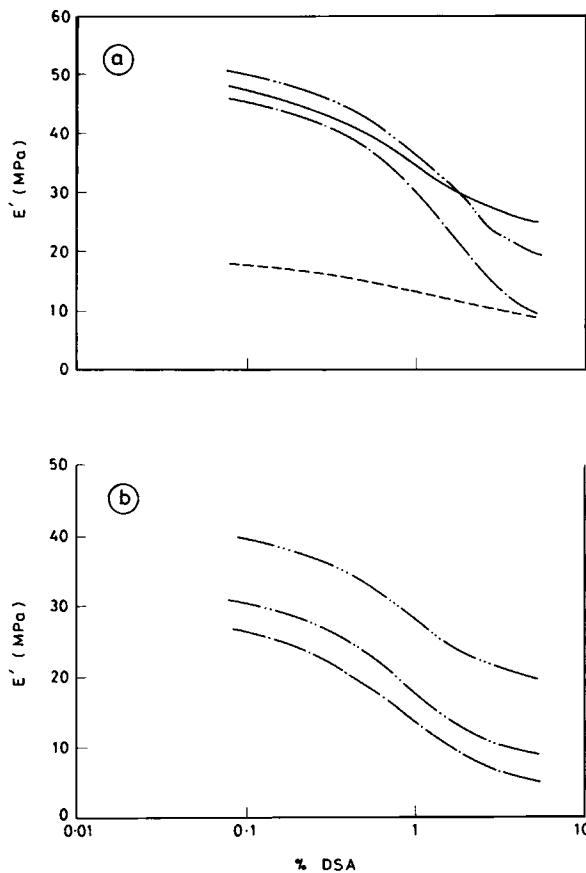


Figure 7 (a) Plot of storage modulus versus %DSA of different XNBR-carbon black mixes, molded for 60 min at 190°C: (— · —) oxidized ISAF carbon black; (— · —) ISAF carbon black; (—) channel black; (---) SRF black. (b) Effect of molding time on the storage modulus versus %DSA plots for XNBR-channel black system (Mix No. 1 of Table II), molded at 190°C: (— · —) 2 min; (— · —) 30 min; (— · · —) 60 min.

Table IV Dynamic Mechanical Properties of Different XNBR–Carbon Black Mixes

Filler Type	Storage Modulus at 0.083% DSA, E'_0 (MPa)	Storage Modulus at 5% DSA, E'_α (MPa)	$\Delta E'$ (MPa)
Oxidized ISAF	55.8	22.0	33.8
ISAF	48.6	8.2	40.4
Channel black	47.1	24.0	23.1
SRF	17.8	7.5	10.3

where σ is the slope of the stress–strain curve in the relatively linear region and η is a carbon–carbon networking factor calculated from the ratio of E' , storage modulus at high DSA and low DSA. A plot of the interaction parameter versus the oxygen content on the surface of the carbon blacks is given in Figure 8a. It is apparent from the plot that the interaction parameter increases linearly with the oxygen concentration on the carbon black surface. Figure 8b shows the variation of the interaction parameter with molding time. Increase in the molding time causes increase in the interaction parameter. The variation of η with the molding time is also included in the figure. With increase in molding time the extent of carbon–carbon networking decreases.

Crosslinking of carboxylic elastomers can be achieved by —OH groups.²³ The presence of —OH groups on the carbon black surface is well established,¹ and the concentration of such groups is expected to be higher in the case of oxidized carbon black. The bound rubber formation takes place due to the physical attachments between the polar groups of the carbon black and the rubber. The weak physical attachments are replaced by strong chemical bonds when the rubber–filler mix is heated to high temperature for prolonged time during molding. Figure 9 depicts a probable mechanism of the rubber–filler bonding.

CONCLUSION

Oxygen containing groups on carbon black surface can chemically bond with the —COOH groups of XNBR and the extent of the reaction depends on the concentration of the oxygen-containing functional groups on the surface of the carbon black. Results of dynamic mechanical studies and measurements of failure properties show that the rein-

Table V Dependence of Dynamic Mechanical Properties of XNBR–Channel Black System (Mix No. 1 of Table II)

Molding Time (min)	Storage Modulus at 0.083% DSA, E'_0 (MPa)	Storage Modulus at 5% DSA, E'_α (MPa)	$\Delta E'$ (MPa)
2	30.4	4.7	25.7
30	34.6	9.8	24.8
60	47.1	24.0	23.1

forcing ability of the surface oxidized carbon black is higher than their nonoxidized counterpart. Measurement of low strain dynamic properties of the molded XNBR–carbon black mixes reveals that

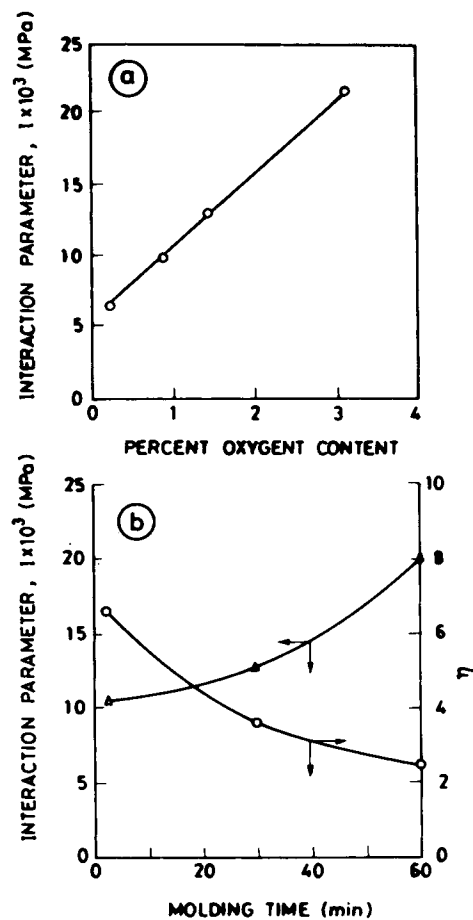


Figure 8 (a) Effect of percent oxygen on the carbon black surface on the interaction parameter (I) of XNBR–carbon black system. (b) Effect of molding time on the interaction parameter (I) and the carbon–carbon networking factor (η) for mix number 1 of Table II.

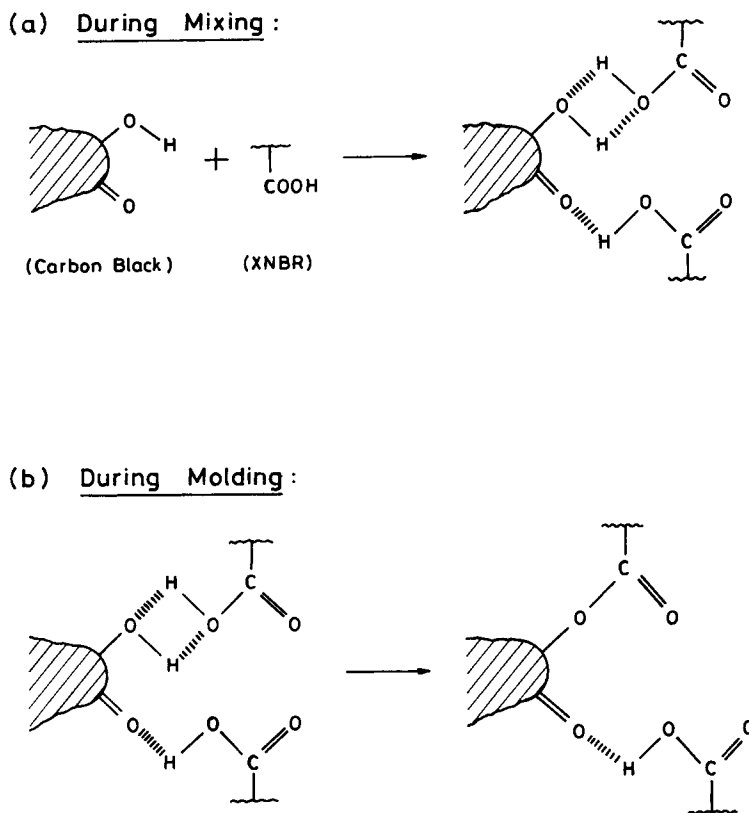


Figure 9 Probable mechanism of bonding between XNBR and oxidized carbon black.

rubber–filler bonding causes reduction in filler–filler interaggregation in the case of the oxidized carbon blacks.

The authors are grateful to Degussa AG, Germany, for kindly providing the carbon blacks used in this study. The financial support of the Department of Science and Technology, Government of India, is also gratefully acknowledged. Thanks are due to Mr. A. Roychoudhury of this center for suggestions.

REFERENCES

1. M. L. Stuebaker, *Rubber Chem. Technol.*, **30**, 1400 (1957).
2. R. C. Bansal, J. B. Donnet, and F. Stoeckli, *Active Carbon*, Marcel Dekker, New York, 1988.
3. J. B. Donnet and A. Vidal, *Adv. Polym. Sci.*, **76**, 103 (1986).
4. M. J. Wang, S. Wolff, and J. B. Donnet, *Rubber Chem. Technol.*, **64**, 714 (1991).
5. G. Kraus, in *Science and Technology of Rubber*, F. R. Eirich, Ed., Academic Press, New York, 1965, Chap. 8, p. 339.
6. G. Kraus, *Angew. Makromol. Chem.*, **60/61**, 215 (1971).
7. A. M. Gessler, *Rubber Age*, **74**, 423 (1953).
8. S. Asai, H. Kaneki, M. Sumita, and K. Miyasaka, *J. Appl. Polym. Sci.*, **43**, 1253 (1991).
9. A. Roychoudhury and P. P. De, *J. Appl. Polym. Sci.*, **50**, 181 (1993).
10. A. Roychoudhury, S. K. De, P. P. De, J. A. Ayala, and G. A. Joyce, *Rubber Chem. Technol.*, **67**, 662 (1994).
11. E. M. Dannenburg, *Rubber Chem. Technol.*, **48**, 410 (1975).
12. E. M. Dannenburg, *Rubber Chem. Technol.*, **59**, 512 (1986).
13. A. I. Medalia, *Rubber Chem. Technol.*, **51**, 437 (1978).
14. N. K. Datta, D. Khastgir, and D. K. Tripathy, *J. Mater. Sci.*, **26**, 177 (1991).
15. A. R. Payne, *J. Appl. Polym. Sci.*, **6**, 57 (1962).
16. A. R. Payne, *J. Appl. Polym. Sci.*, **7**, 873 (1963).
17. A. R. Payne, *J. Appl. Polym. Sci.*, **9**, 2273 (1965).
18. M. L. Stuebaker and J. R. Beatty, *Rubber Chem. Technol.*, **47**, 803 (1974).

19. M. G. Huson, W. J. McGill, and P. J. Swart, *J. Polym. Sci., Polym. Lett. Ed.*, **22**, 143 (1984).
20. A. R. Payne and R. E. Whittaker, *Rubber Chem. Technol.*, **44**, 440 (1971).
21. A. R. Payne and R. E. Whittaker, *J. Appl. Polym. Sci.*, **16**, 1191 (1972).
22. J. A. Ayala, W. M. Hess, G. A. Joyce, and F. D. Kistler, *Rubber Chem. Technol.*, **66**, 772 (1993).
23. H. P. Brown, *Rubber Chem. Technol.*, **36**, 931 (1963).

Received September 15, 1994

Accepted February 28, 1995